Materials Horizons

A Surprisingly Gentle Approach to Cavity Containing Spherocylindrical Microparticles from Ordinary Polymer Dispersions in Flow

Journal:	*Materials Horizons*
Manuscript ID	MH-COM-07-2021-001108.R1
Article Type:	Communication
Date Submitted by the Author:	19-Aug-2021
Complete List of Authors:	Tripathi, Amit; University of New Hampshire, Chemistry Tsavalas, John; University of New Hampshire, Chemistry; University of New Hampshire, Materials Science Program

COMMUNICATION

A Surprisingly Gentle Approach to Cavity Containing Spherocylindrical Microparticles from Ordinary Polymer Dispersions in Flow†

*Amit K. Tripathi[1] and John G. Tsavalas[1,2]**

[1]Department of Chemistry, University of New Hampshire, Durham, NH 03824, USA
[2]Materials Science Program, University of New Hampshire, Durham, NH 03824, USA
*E-mail: john.tsavalas@unh.edu
ORCIDs: A.K.T. (0000-0003-1411-3746), J.G.T. (0000-0003-4955-9991)

†Electronic supplementary information (ESI) available: This includes full synthetic methods, additional conditions and characterizations.

Keywords: spherocylinder, hollow, capsule, plastic deformation, morphology, glassy polymer

Abstract

Herein, we demonstrate a facile approach to fully transform spherical polymeric microparticles to elongated spherocylinders containing an internal cavity under ambient and mild stirring conditions. Critical to the process is to deform the amorphous and non-crosslinked particles under glassy conditions for an unusually long time; 120 hours for the poly(styrene-co-glycidyl methacrylate) microparticles discussed in greatest detail. Larger particles in the 5-micron and greater range were markedly more susceptible to the shear imposed by stirring the aqueous dispersion. The resulting morphology is robust and kinetically frozen yet reverts to the original spherical shape if annealed above the glass transition temperature with suitable temperature or plasticizer. The volume fraction of the internal void can be modulated by particle composition and process conditions and is irregular in shape we believe as a result of a cavitation event during plastic deformation.

New concepts

Contrary to most approaches leveraging plasticization to manipulate polymeric microparticles into aspherical morphologies, we demonstrate here a rather facile process toward a uniform conversion

of spheres to spherocylinders under glassy conditions. Moreover, as a result of leveraging plastic deformation, the spherocylindrical form contains a microcavity suited to optical applications or loading of the capsules with payload. The spherocylindrical morphology also matches with sought after models for low Reynolds number flow shapes commonly observed with swimming bacterium – this shape has promise for a wide variety of materials applications. A surprising advantage in our approach is that this well-defined morphological transition results from glassy plastic deformation at room temperature and merely as a result of imposing shear to orient the particles in the dispersion via mild stirring – very accessible and inexpensive process conditions. No special plasticizer is necessary, and in fact when plasticization was present the morphology was lost with a reversion back to the lower energy spherical state. While conditions shown here required circa 120 hours for complete conversion, we anticipate the time necessary, and the characteristics of the internal cavity, able to be modulated by primary particle size, hydrodynamic flow conditions, and the balance between particle and continuous phase viscosity.

Introduction

The isotropy of a sphere pervades the morphology dominantly observed in amorphous polymer dispersions. Polymer particles are ubiquitous in materials science applications such as photonic crystals[1-4], ionic solids[5], energy storage and electrodes[6], biomedical, biocatalysis, and drug delivery applications[7-9], through to well-known commodity products such latex particles within architectural paints. The reason the spherical morphology dominates is simple. It is a thermodynamically driven process toward reduction of the interfacial tension between a dispersed non-polar phase and its engulfing polar continuous phase (or vice versa); the sphere provides the minimum exposed surface area. These spheres are typically built either via an accretion based synthetic process born from a nucleation site or from a similar evolution but with phase mixing and continuous rearrangement through a phase separation process (e.g. emulsion polymerization,

dispersion polymerization, and suspension polymerization). Again, for reasons of minimization of external surface area, a densely packed arrangement resulting in a solid sphere is normally observed. Elaborate processes exist to impose a hollow interior to such particles for optical applications[10,11], deformability of the spheres[12-15], or to generate a container encapsulating a liquid or otherwise payload[16-19].

Processes also exist, both via reaction and post-reaction modifications, to generate elongated or cylindrical shaped particles. Several approaches have been reported in the literature such as those that leverage synthetic strategies[20-22], non-wetting template molding[23,24], microfluidics[25-27] and mechanical stretching[28-31] to describe means to obtain elongated non-spherical particles. In general, these procedures are either very complex or require multiple steps to obtain the final morphology. Here, we instead report on a facile method to simultaneously produce both a non-spherical shape as well as a voided interior in dispersed polymer particles. While the relevant process conditions are mild and do not require expensive or complex reagents, the conditions themselves are surprisingly nonintuitive.

Prototype System

The appearance of spherocylindrical particles was observed serendipitously during an attempt to surface functionalize micron-sized poly(styrene-co-glycidyl methacrylate), poly(STY-co-GMA), with ethylenediamine (EDA). While the original intent was simply to install an amine functionality onto the particle surface for subsequent reactions, a morphological transformation of the primary particles was not expected. It is important to note here at the onset that we ultimately found that the resulting elongated particle shape is not related to any reaction pathway (e.g. EDA reaction with GMA), but rather simply a deformation process that relates to the particle size and malleability. It will later be shown that EDA and GMA can be removed, yet this first system serves as our control prototype that inspired the work. The primary poly(STY-co-GMA), 75/25 wt/wt particles were produced by dispersion polymerization in ethanol using poly(vinylpyrrolidone) (PVP360, Mw 360,000 g/mol) as a stabilizer and azobisisobutyronitrile (AIBN) as initiator. The resulting spherical particles were highly polydisperse with particle sizes ranging from 0.8 μm to 13 μm; a common issue for the case of dispersion copolymerization.[32-34] The ethanol, along with free PVP360, was replaced with deionized (DI) water by multiple centrifugation-redispersion cycles, which also removed particles smaller than 5 μm as confirmed by scanning electron

microscopy (SEM) (Figure 1a, with examples of the spherical morphology colored in red). For the next step, excess EDA (~32:1 mol EDA per GMA, so as to prevent crosslinking) was added to a 1 wt% aqueous dispersion of these cleaned particles and suspended in an oil bath at 70 ˚C for 18 hours.

Under an optical microscope, it was found that a fraction of the originally spherical particles had transformed into obround shapes during this process; two semicircles connected by extended parallel lines tangent to the endpoints in 2D, or a spherocylinder in 3D (Figure 1b). This observation was verified by multiple reproductions of the experiment. Furthermore, we observed a dark spot in the middle of each spherocylindrical particle whose origin was rather unclear; only the obround spherocylindrical particles contained such a defect, where residual spheres remained entirely uniform. The sample was further investigated under SEM where the observation of spherocylindrical particles was additionally corroborated (Figure 1c, with green and blue coloring of the cylindrical portion of certain particles for emphasis). Not all spheres transformed to spherocylinders and the long axis was also not uniform in length for all such particles. Moreover, the rounded spherical caps only approached hemispheres for very short cylindrical extension while

the cap height reduced with increasing cylindrical elongation. From Figure 1c, we can see that the cylindrical portion of those particles also exhibits a smooth continuous external surface suggesting the anomaly observed from optical images (Figure 1b) is due to internal morphology. To reveal the interior, the two blue colored particles in Figure 1c were ablated using a focused ion beam (FIB) within the SEM, as shown in Figure 1d. Confirming the interpretation of the dark spot in Figure 1b to be due to internal reflection of light, the spherocylindrical particles indeed contained an internal void.

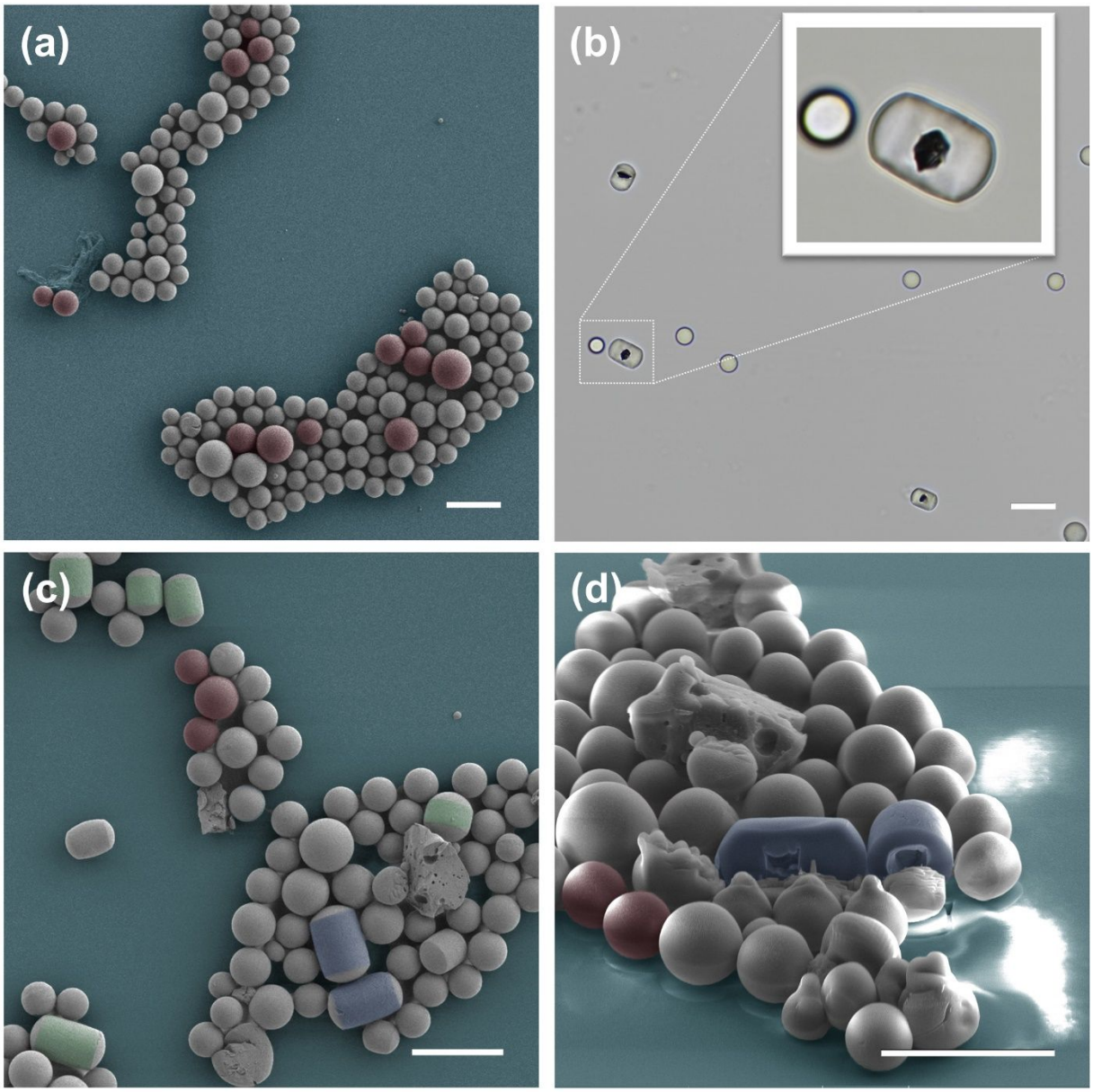

Figure 1. **(a)** Scanning electron microscopy (SEM) image of poly(STY-co-GMA) particles prepared by dispersion polymerization, with example spherical particles false colored in red. **(b)** Optical microscope image of the same particles after exchanging ethanol for water, removing excess PVP, and stirring at 70 ˚C for 18 hrs. Magnified selection shows only those particles that transformed to obround shapes contain a dark feature in the particle center. **(c)** SEM of the same sample false colored with both green and blue to emphasize the elongated center of the spherocylinders formed (examples particles that remained spherical in red). **(d)** 90˚ rotated SEM

image of the same sample after focused ion bean ablation of the blue colored particles to reveal their hollow interior. The size bar in each image represents 20 μm.

Probing Chemical Reaction or Physical Property Dependence

Returning to the conditions that produced the unexpected morphological transformation, addition of EDA while stirring at elevated temperature for extended time, we attempted to systematically explore the relevant chemical and process conditions. We expected the stirring temperature, that temperature relative to the polymer glass point in particular, to be a key parameter governing the susceptibility of particles to deformation. To minimize variables and to produce a simplified control experiment, we substituted ethyl methacrylate (EMA) for the original GMA content (copolymer ratio and dispersion polymerization reaction conditions the same) to maintain effective glass point without reactive functionality, but now without new reagent addition or pH change (i.e. no EDA was added) post-polymerization. After exchanging the ethanol content for water and removal of excess PVP, the stirring temperature for this control experiment was set to room temperature (30 °C). At approximately 40 °C below the polymer glass transition (T_g, see Figure S1), also 40 °C below the temperature employed for the system in Figure 1, the glassy particles were expected to remain spherical.

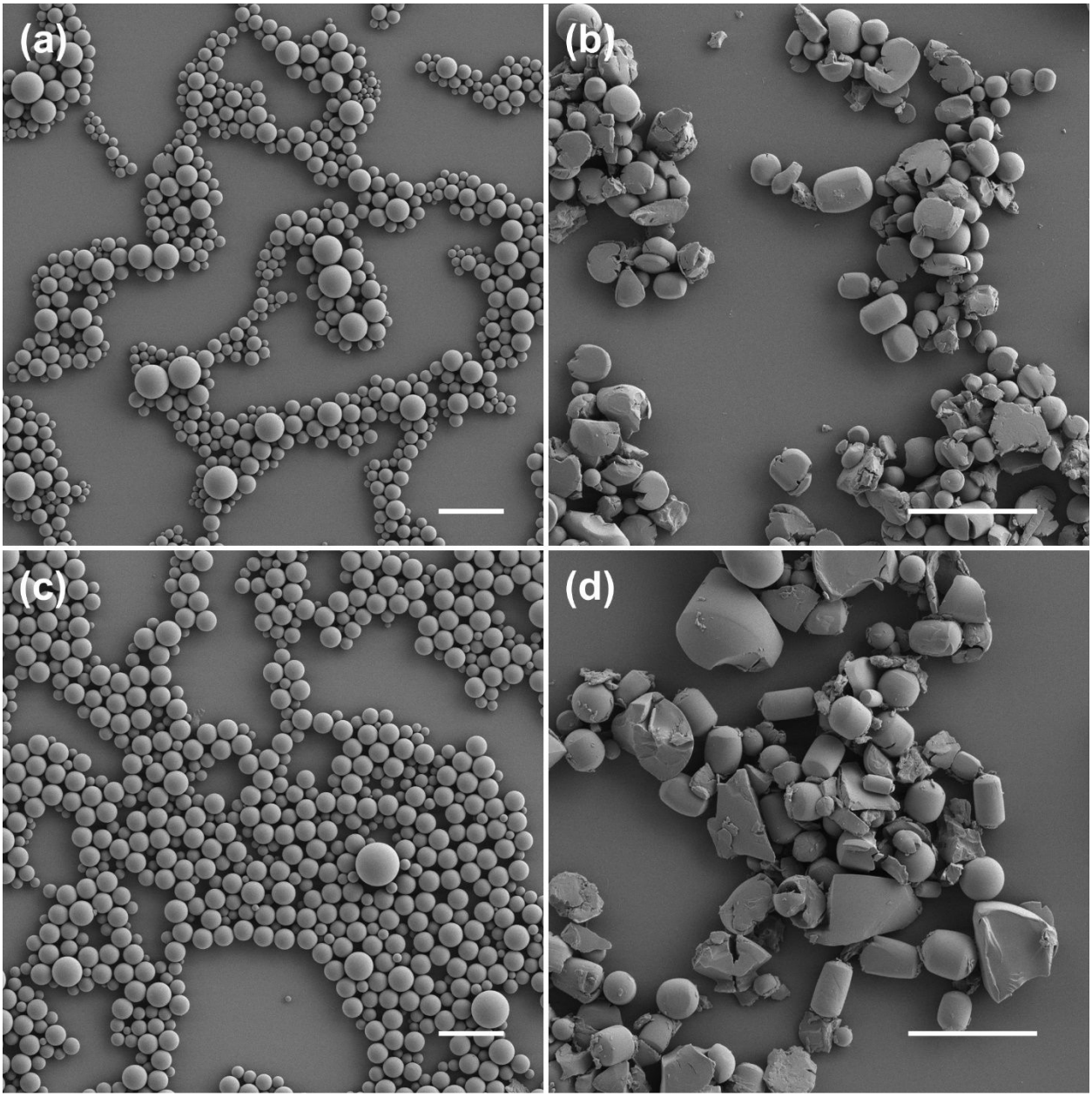

Figure 2. **(a)** Scanning electron microscopy (SEM) image of poly(STY-co-EMA) particles prepared by dispersion polymerization, **(b)** SEM image of the same particles after exchanging ethanol for water, removing excess PVP, and stirring at 30 ˚C for 120 hours, **(c)** SEM image of poly(STY-co-MMA) particles prepared by dispersion polymerization, **(d)** SEM image of the same particles after exchanging ethanol for water, removing excess PVP, and stirring at 30 ˚C for 120 hours. The size bar in each image represents 20 μm.

To our surprise, even under quite glassy conditions, only in water with surfactant removed, no reactive functionality on the particles (e.g. GMA), and no pH change or reactive component addition (e.g. EDA), a significant portion of spherocylinders were again observed (transformation of Figure 2a to 2b). Where conditions in Figure 1 were only for 18 hours, here at 120 hours of stirring, under glassy conditions, an apparent rupture of larger particles in the sample was also observed (Figure 2b). As this is a flow process, there is larger distortion of flow path around larger objects and as such, those larger particles are more susceptible to elongation. Figure 2a shows a wide as-synthesized particle size distribution, not uncommon for dispersion copolymerization, where the largest particles observed suffered rupture by overextending their equatorial axis during flow for extended time (Figure 2b). With the internal cavity formation noted it is not surprising that at some point during elongation the mechanical integrity of the shell could fail. The particle rupture is most often nearest the elongated particle center axis as the void in Figure 1b would suggest thinning of the shell to be most dramatic there, and clearly confirmed in supplemental Figures S2b and S2c even at only 24 hours into the process. Intact spherocylindrical particles are indeed also observed, derived from smaller initial dimensions. The susceptibility of smaller

spheres to the flow induced orienting effect should be less pronounced under similar flow conditions and thus may require more time to deform (or ultimately potentially rupture). Alternatively, those smaller spheres may not sufficiently distort the flow path under laminar conditions to produce shear suited to deformation (see also Supplemental Figure S2 for the same system, which still clearly shows smaller spherocylinders intact, as well as even smaller spheres still undistorted).

A variation was then produced substituting methyl methacrylate (MMA) for the EMA content, again leveraging the same copolymer ratio and overall polymerization conditions, while here the effective polymer glass point would be approximately 70 ˚C higher than room temperature during stirring over extended time. It should be noted that all copolymerizations discussed here were observed to have narrow glass transitions by DSC analysis (See Figures S1 and Figure 6) confirming statistical copolymers were formed without compositional drift regardless of the comonomer polymerized with styrene in these cases (otherwise transition width would be

dramatically greater). Once again, now with MMA as the comonomer, spherocylindrical particles resulted from the plastic deformation under flow (transformation of Figure 2c to 2d). Compared to the EMA containing case, poly(STY-co-MMA) produced significantly larger primary particles (some approaching 20 microns) and thus at equivalent stirring time it is not surprising that more significant rupture was observed (after 120 hours) for the largest particles in Figure 2d.

Contrasting the three copolymerizations of styrene with either GMA, EMA, or MMA, and notably without any reactive additives (such as EDA), the external particle morphology transformation appears not to be compositionally dependent and instead a general feature of slow plastic deformation under flow. In Figure 3, the internal morphology of the most glassy poly(STY-co-MMA) case was evaluated both by optical microscopy (inset) and SEM where focused ion beam etching of the particles again confirmed the development of an internal void resulting from the elongation process during stirring. The external and internal morphological features were retained once removed from flow as the polymer was always in a glassy state.

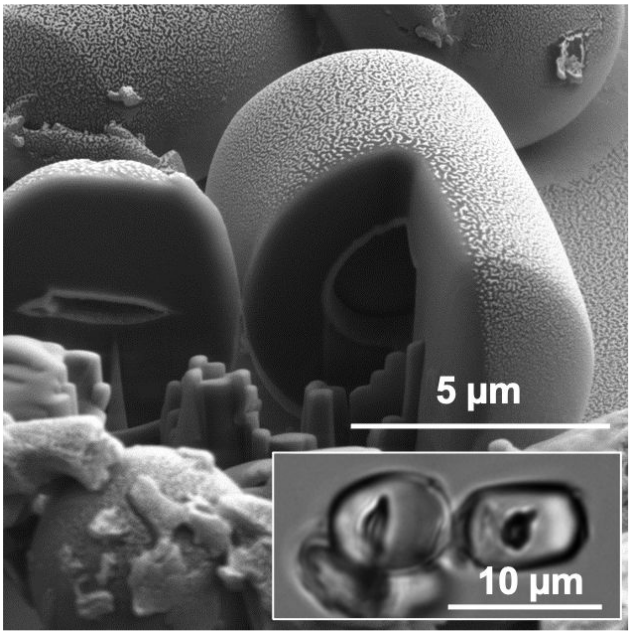

Figure 3. Scanning electron microscopy image of approximately 10 µm sized poly(STY-co-MMA) particles after 120 hours of stirring at room temperature with focused ion beam etching to reveal the internal particle morphology and with inset image from optical microscopy corroborating the internal particle void.

Probing Primary Particle Elongation vs. Multi-Particle Aggregation

With reproducibility established for both external and internal morphology for several variations in composition and physical properties, we turned to question whether the spherocylindrical morphology was a result of multi-particle aggregation and subsequent annealing of those oligoclusters (under flow, as the MMA and EMA cases were glassy), or if the transformation was indeed that of individual particles. As evident in Figures 1a, 2a, and 2c, the dispersion copolymerizations led to highly polydisperse particle size. This then resulted in spherocylindrical

particles of varying size and aspect ratio. In attempt to reduce the variables at play to better probe the mechanism of formation, we aimed to reproduce the same reaction conditions but with a more monodisperse primary particle size.

To do so, a two-step process was employed to yield monodisperse poly(STY-co-GMA) particles of the same compositional ratio, now via seeded dispersion polymerization.[35,36] A poly(styrene) seed (~120 nm) was first produced by emulsion polymerization and cleaned using an ion exchange resin to remove all unbound ionic species such as surfactant and initiator. After the subsequent growth by dispersion polymerization, followed by multiple centrifugation-redispersion cycles, the particles obtained resulted in a monodispersed spherical diameter of 5.56 μm (Figure 4a). Based on what was observed for significantly larger particles in Figure 2, this was deemed to be a good size range to probe the dynamics of the morphology transformation with less chance of particle rupture.

Now with a monodisperse system, focus could be placed on the physical transformation of the particles without concerns for influence of particle size variations. In a 20 mL scintillation vial, 3

grams of the monodisperse aqueous dispersion of poly(STY-co-GMA) polymer particles (solids content 2 wt%) were added and stirred at room temperature at 750 RPM with samples taken periodically for temporal characterization. Corroborating the poly(STY-co-EMA) and poly(STY-co-MMA) glassy conditions in Figure 2 also performed at room temperature, spherocylindrical particles were again observed (Figures 4b-f). In fact, the fraction of elongated particles increased with time and after 120 hours, nearly all the spherical particles were converted to the spherocylindrical morphology (here without rupture, due to the smaller particle size). For quantitative analysis, each SEM image was analyzed to count the total number of spherocylindrical and spherical particles. In Figure 5a, the estimated fraction of spherocylindrical particles generated vs stirring time is plotted and we find that this transformation proceeds nearly linearly (up to 96 hours) at room temperature; under strongly glassy conditions. One would expect the shear flow paths around larger particles to be the most distorted and thus once a random deformation event initiates, a faster elongation step likely occurs; a popcorn effect of sorts. Likewise, the susceptibility of smaller spheres to this orienting effect should be less pronounced under the same flow conditions and thus may require more time (consistent with a persistence of smaller spheres in all cases above, while the largest of the populations in Figure 2 suffered rupture). However, in

this more monodispersed seeded dispersion polymerized case, the size deviations are more subtle leading to apparent linearity in transformation time emphasizing the randomness of the onset of deformation for that particular size. We should emphasize that this shape transformation experiment took 5 days of continuous stirring to complete, with less than 20% of the original spheres impacted over the first 24 hours. While the process conditions are quite common, the duration of time for the change renders this effect easy to go unnoticed.

Along with elongated features, the other observation noted earlier in Figures 1b, 1d, and 3 was the presence of a void within the spherocylindrical particles. As none of the residual spheres in Figure 1b were noted to contain this feature, we felt the volume displaced in the interior to generate the void might help ascertain as to whether the transformation was due to an intraparticle or interparticle event. To address this query, the complete dimensions of approximately 250 spherocylindrical particles in the SEM images obtained for the 120-hour sample (e.g. Figure 4f) were estimated. From these, we deduced the volume distribution of the spherocylindrical particles (see Supplemental Section S2) and compared that with the volume distribution from the same process imposed on the original spherical particles (e.g. Figure 4a). From Figure 5b, it is evident

that the volume of spherocylindrical particles is roughly 1.1 times larger than the volume of original spherical particles. With only an approximate 10% volumetric internal void, and starting from monodisperse spheres, these calculations also indicate that the spherocylindrical particles are indeed formed from individual spherical particles and cannot be from an aggregation of two or more particles. With only one non-spherical morphology observed, this is also consistent with the fact that the original particles are isotropic and would not have any directional assembly tendency.

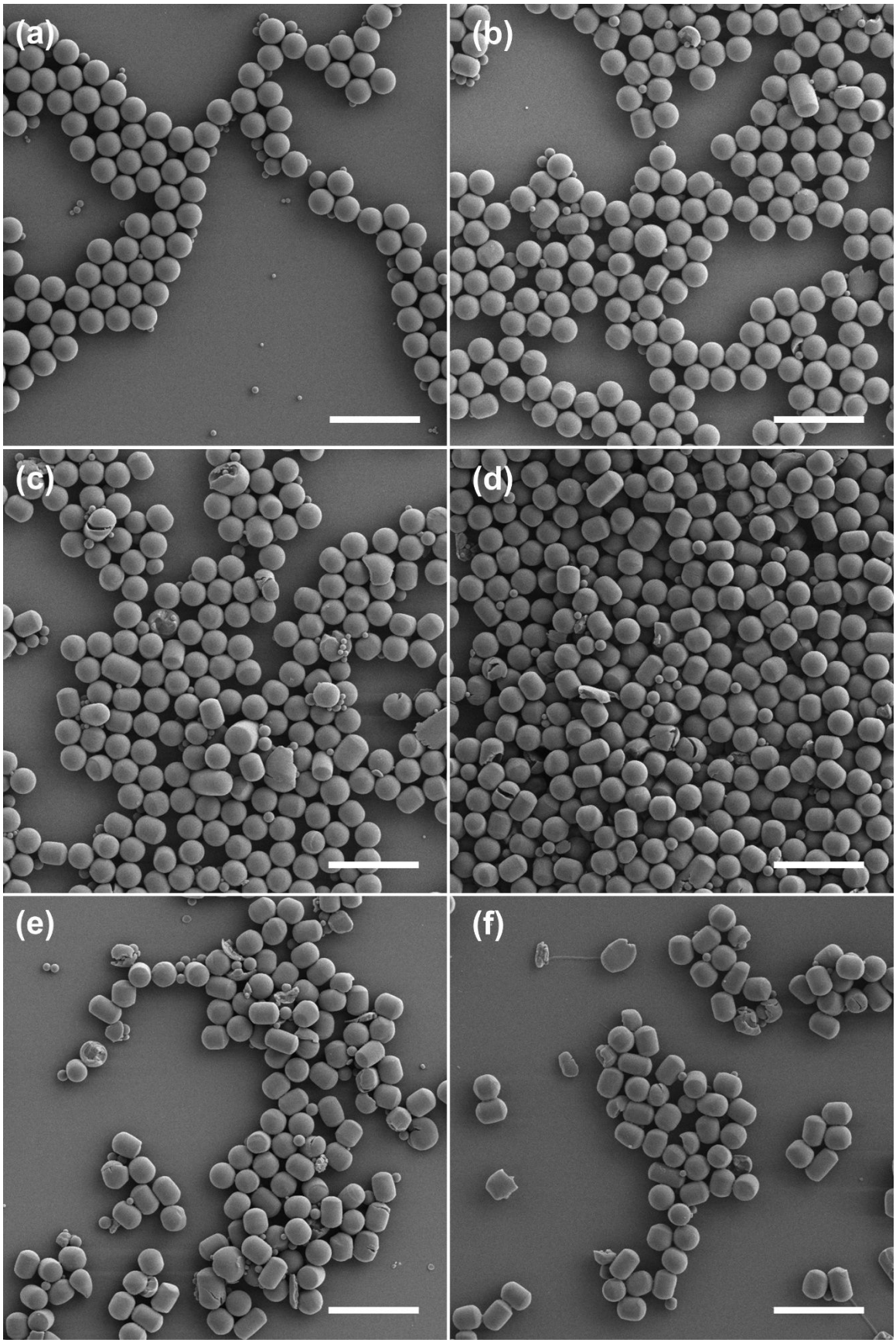
(a)
(b)
(c)
(d)
(e)
(f)

Figure 4. Monodisperse 5.56 μm primary particles produced by seeded dispersion polymerization **(a)** and the progression of their transformation to spherocylinders at room temperature with no other reactant for stirring times of 23 hrs **(b)**, 48 hrs **(c)**, 70 hrs **(d)**, 96 hrs **(e)**, and 120 hrs **(f)**. All scale bars represent 20 microns.

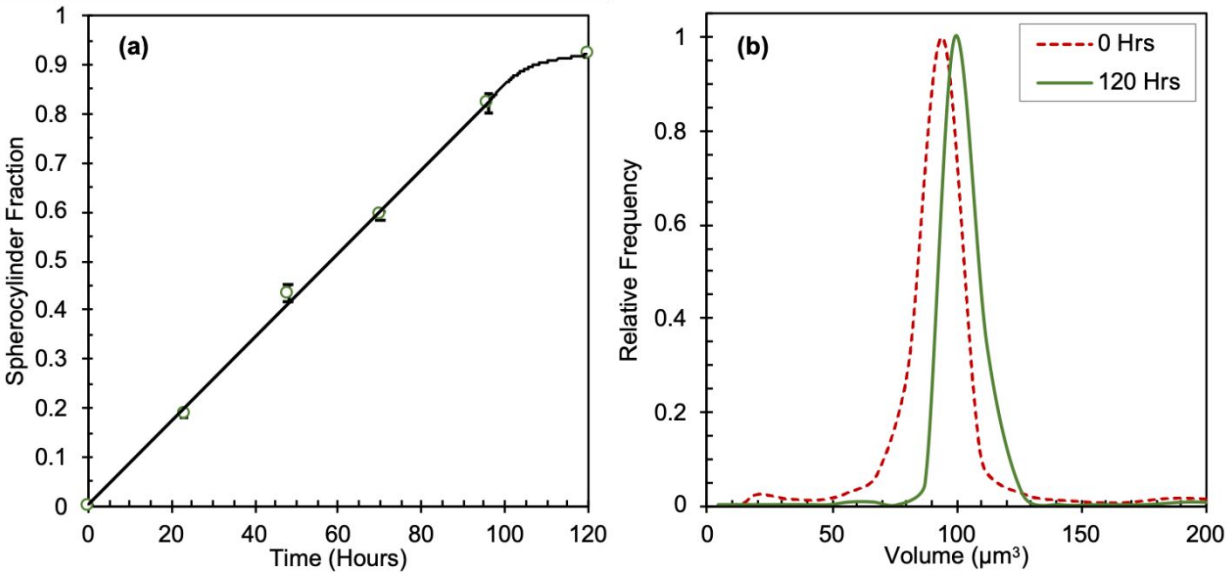

Figure 5. Quantitative analysis from SEM images of the ratio of spherocylinder to spherical morphology versus stirring time at room temperature **(a)** and volume distribution comparison for the 120-hour sample of spherocylinders versus the original dispersion of spheres **(b)**

Potential for Plasticization & Reversibility of Elongation

Now established that the spherocylinders result from an individual intraparticle transformation, we return to the question of malleability of the particles which we certainly expected to be quite rigid, glassy at room temperature, and thus unlikely to be easily deformed. To more directly confirm whether there are any unforeseen low T_g regions in the particles, differential scanning calorimetry

was performed on the polymer particles in both the dry and fully hydrated state.[37] The fully dried poly(STY-co-GMA) system showed a glass transition of 91 ˚C in Figure 6 (solid curve), and when analyzed in the fully hydrated state (from a sample of the dispersion itself just prior to stirring at room temperature[38]) we observe the hydroplasticized glass transition to be 72 ˚C (blue dashed curve). This is still roughly 47 ˚C higher than the room temperature used for the experiments that led to the morphological transformation and there are no detectable low Tg signals in either profile. The derivative of the reversing heat capacity is shown as it more clearly reveals not only the glass transition temperature, without influence of the enthalpy of relaxation, but also its distribution and width of transition (the 20˚ width also confirms statistical copolymerization and indicates a homogeneous particle composition system).[39] The full temperature scan for these analyses started as low as -20 ˚C, as seen in Figure S4, yet the enthalpy of melting for the water dominates the signal until 10 ˚C.[38]

This suggests that the spherocylindrical particles formed during the stirring process are kinetically frozen and deformed under highly glassy conditions at room temperature. Plastic deformation is often applied to manipulate polymeric macroscopic shapes for both semi-crystalline[40,41] and elastic

materials[42,43], yet we believe it may be the appropriate description for what we are observing here even though our polymers are amorphous and non-crosslinked. Deformation of a glassy amorphous polymer is not a new concept in itself[44] however the underlying theoretical mechanisms are still being developed[45-47] and we are not aware of this process being applied to influence polymer particle morphology. In this work, the resistance to deformation is the surface energy penalty when the particle shape becomes anisotropic. The same transformation was observed when performed at 70 ˚C (Figure 1), which coincidentally is also the peak of the wet Tg profile of the polymer (Figure 6). It therefore begged the question as to what would happen if the sample were heated to a temperature sufficiently above the effective glass transition to allow polymer chain rearrangement, if a driving force for doing so remains.[43,48] To probe this, the sample obtained after 48 hours at room temperature (Figure 4c) was heated to 90 ˚C for 6 hours. At approximately 20 ˚C above the wet Tg, the polymer would certainly not be glassy and any morphological rearrangement towards energy minimization should be possible.[49] Indeed, in Figure 7a, we find that all the elongated particles had reverted back to spherical particles, yet some degree of aggregation and coalescence was observed as the annealing was performed without any new stabilizer addition. When the same annealing experiment was repeated, but with the addition of sodium dodecyl

sulfate (SDS) surfactant near the critical micellar concentration (CMC), it is overwhelmingly clear in Figure 7b that after heating the system above the Tg, the spherocylindrical morphology is lost and all particles regain sphericity; the lowest surface energy morphology. It was at this point that we found that another group had recently explored a similar system, however their claim was that susceptibility of the spheres to elongation was due to the sample being plasticized by excess PVP stabilizer.[50] While we could indeed reproduce their conditions (Figure S5), plasticization cannot be the enabling factor for this type of morphological change. We have shown that we observe the transformation when our particles are clearly in a glassy state, without any excess PVP, and if indeed plasticized they were found to regress back to spheres. Minami et al. also did not observe a hollow particle interior, yet their poly(styrene) particles were only 1.5 microns and may not have been affected by the process conditions to the extent that our 5+ micron particles were.[42]

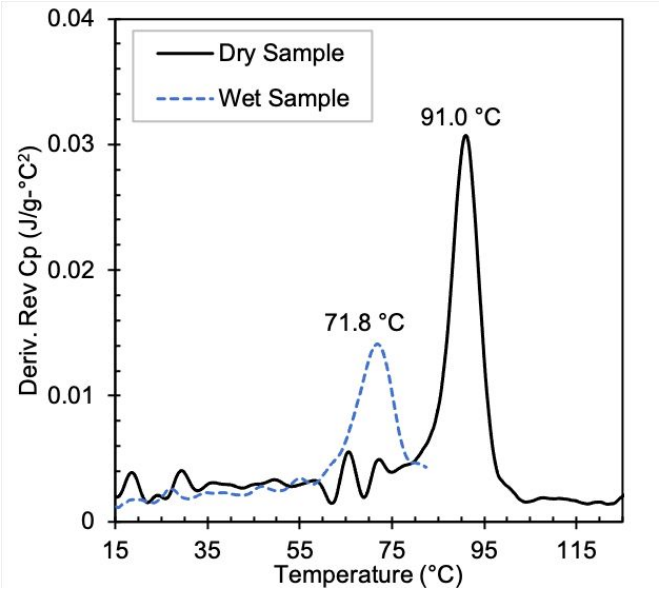

Figure 6. Modulated differential scanning calorimetry analysis of the poly(STY-co-GMA) polymer in both the fully dried (solid profile) and hydrated dispersion (dashed profile) state. The derivative of the reversing heat capacity is shown as it more clearly reveals not only the glass transition temperature but also its distribution and width of transition

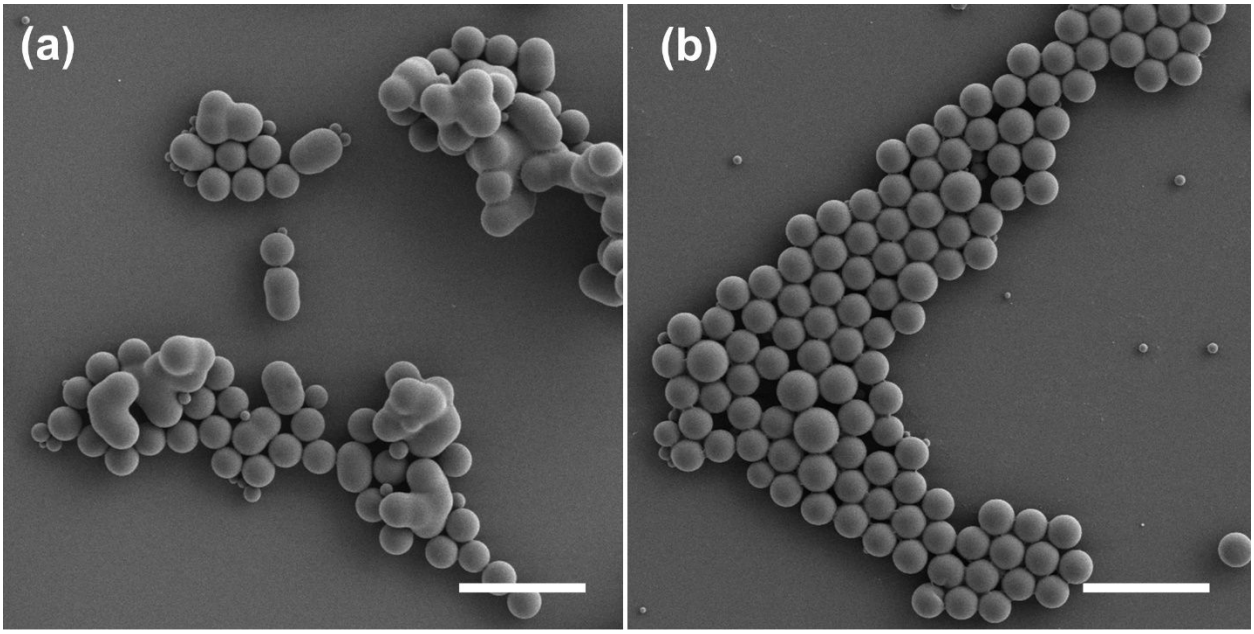

Figure 7. SEM of sample from Figure 4c heated to 90 ˚C for 6 hours **(a)**, and same sample annealed in same fashion but after addition of SDS for colloidal stability **(b)**. All scale bars are 20 microns.

DISCUSSION

Based on the observations reported here, the proposed mechanism for the formation of spherocylindrical hollow particles from spheres is by the shear imposed on them during vigorous stirring under laminar conditions (common magnetic stirbar). Interestingly, this shear is effective on multi-micron sized particles even under highly glassy conditions. The non-spherical nature of the internal void (in Figure 1b and 1d) is further consistent evidence of shear and flow induced deformation. We believe this void may be a result of cavitation within the particles during deformation after sufficient extension of the equatorial region of the cylinder.[51-53] A key parameter at play here appears to be the primary particle size[42] and the viscosity of the continuous medium versus the glassy dispersed phase.

Variations of the conditions described here were also explored. When the particles were synthesized with a stabilizer other than PVP360 (poly(acrylic acid), Mw 50k g/mole, Figure S6), the transformation to spherocylindrical morphology was still observed, again under the same mild conditions stirring at room temperature without additives after cleaning and exchanging the

continuous phase to water. As a point of emphasis relating to the importance of particle size, one can easily see the susceptibility of the larger particles (Figure S6 c,d) to this transformation as the primary particle size distribution (Figure S6 a,b) was so polydisperse; spheres even in the 5 micron range did not appear to deform under these conditions or timeframe (117 hrs), while larger particles did transform to spherocylinders akin to those reported above. We also performed a variation of the experiment shown in Figure 7, but at room temperature and with the addition of styrene monomer as a plasticizer. Even after only 4 hours, the reversion of spherocylinders back to spheres was again observed. Finally, the cleaned and solvent exchanged aqueous dispersions were also held unstirred as a control on the shelf. Observed periodically over a two-month period by optical microscopy, they were found to remain exclusively spherical. Many variations of process and composition remain to be explored, yet this nonintuitive slow transformation to a distinct non-spherical shape presents an intriguing and mild method for morphological manipulation.

Author contributions

A.K.T. and J.G.T conceptualized the study. A.K.T conducted the synthetic and analytical investigation. A.K.T and J.G.T interpreted experimental results and equally contributed to the visualization, writing, review and editing.

Acknowledgments

This research is supported by NH BioMade under a National Science Foundation EPSCoR award (#1757371). The authors are very appreciative of Laura Bicknell for her help in adding color emphasis to the SEM images. We are also grateful to the University of New Hampshire Instrumentation Center (UIC), and specifically Nancy Cherim for her aid with focused ion beam samples in the SEM and Dr. Mark Townley for confocal microscopy help and discussions.

Conflicts of Interest

There are no conflicts to declare.

References

1 D. K. Rhee, B. Jung, Y. H. Kim, S. J. Yeo, S. Choi, A. Rauf, S. Han, G. Yi, D. Lee and P. J. Yoo, *ACS Appl. Mater. Interfaces*, 2014, **6**, 9950.

2 C. E. Reese, A. V. Mikhonin, M. Kamenjicki, A. Tikhonov and S. A. Asher, *J. Am. Chem. Soc.* 2004, **126**, 1493.

3 J. Ge and Y. Yin, *Angew. Chem., Int. Ed. Engl.*, 2011, **50**, 1492.

4 V. L. Colvin, *MRS Bull.*, 2001, **26**, 637.

5 T. Hueckel, G. M. Hocky, J. Palacci and S. Sacanna, *Nature*, 2020, **580**, 487.

6 S. Srivastava, J. L. Schaefer, Z. Yang, Z. Tu and L. A. Archer, *Adv. Mater.*, 2014, **26**, 201.

7 M. A. C. Stuart, W. T. S. Huck, J. Genzer, M. Müller, C. Ober, M. Stamm, G. B. Sukhorukov, I. Szleifer, V. V. Tsukruk, M. Urban, F. Winnik, S. Zauscher, I. Luzinov and S. Minko, *Nat. Mater.*, 2010, **9**, 101.

8 Q. Guo, C. J. Bishop, R. A. Meyer, D. R. Wilson, L. Olasov, D. E. Schlesinger, P. T. Mather, J. B. Spicer, J. H. Elisseeff and J. J. Green, *ACS Appl. Mater. Interfaces*, 2018, **10**, 13333.

9 F. Caruso, *Adv. Mater.*, 2001, **13**, 11.

10 K. Zhou, L. Tong, J. Deng and W. Yang, *J. Mater. Chem.*, 2010, **20**, 781.

11 S. Nuasaen and P. Tangboriboonrat, *Prog. Org. Coatings*, 2015, **79**, 83.

12 C. J. McDonald and M. J. Devon, *Adv. Colloid Interface Sci.*, 2002, **99**, 181.

13 V. N. Pavlyuchenko, O. V. Sorochinskaya, S. S. Ivanchev, V. V. Klubin, G. S. Kreichman, V. P. Budtov, M. Skrifvars, E. Halme and J. Koskinen, *J. Polym. Sci. Part A Polym. Chem.*, 2001, **39**, 1435.

14 W. Wichaita, D. Polpanich and P. Tangboriboonrat, *Ind. Eng. Chem. Res.*, 2019, **58**, 20880.

15 E. Donath, G. B. Sukhorukov, F. Caruso, S. A. Davis and H. Möhwald, *Angew. Chemie Int. Ed.*, 1998, **37**, 2201.

16 J. Cui, Y. Wang, A. Postma, J. Hao, L. Hosta-Rigau and F. Caruso, *Adv. Funct. Mater.*, 2010, **20**, 1625.

17 X. Yang, L. Chen, B. Han, X. Yang and H. Duan, *Polymer (Guildf).*, 2010, **51**, 2533.

18 C. Mangeney, S. Bousalem, C. Connan, M.-J. Vaulay, S. Bernard and M. M. Chehimi, *Langmuir*, 2006, **22**, 10163.

19 S. R. White, N. R. Sottos, P. H. Geubelle, J. S. Moore, M. R. Kessler, S. R. Sriram, E. N. Brown and S. Viswanathan, *Nature*, 2001, **409**, 794.

20 A. Kuijk, A. van Blaaderen and A. Imhof, *J. Am. Chem. Soc.*, 2011, **133**, 2346–2349.

21 J.-W. Kim, R. J. Larsen and D. A. Weitz, *J. Am. Chem. Soc.*, 2006, **128**, 14374–14377.

22 C. Wei, A. Plucinski, S. Nuasaen, A. Tripathi, P. Tangboriboonrat and K. Tauer, *Macromolecules*, 2017, **50**, 349–363.

23 H. Zhang, J. K. Nunes, S. E. A. Gratton, K. P. Herlihy, P. D. Pohlhaus and J. M. DeSimone, *New J. Phys.*, 2009, **11**, 075018.

24 J. P. Rolland, B. W. Maynor, L. E. Euliss, A. E. Exner, G. M. Denison and J. M. DeSimone, *J. Am. Chem. Soc.*, 2005, **127**, 10096–10100.

25 D. Dendukuri, S. S. Gu, D. C. Pregibon, T. A. Hatton and P. S. Doyle, *Lab Chip*, 2007, **7**, 818.

26 D. Dendukuri, K. Tsoi, T. A. Hatton and P. S. Doyle, *Langmuir*, 2005, **21**, 2113–2116.

27 S. Xu, Z. Nie, M. Seo, P. Lewis, E. Kumacheva, H. A. Stone, P. Garstecki, D. B. Weibel, I. Gitlin and G. M. Whitesides, *Angew. Chemie Int. Ed.*, 2005, **44**, 724–728.

28 J. A. Champion, Y. K. Katare and S. Mitragotri, *Proc. Natl. Acad. Sci.*, 2007, **104**, 11901–11904.

29 Z. Zhang, P. Pfleiderer, A. B. Schofield, C. Clasen and J. Vermant, *J. Am. Chem. Soc.*, 2011, **133**, 392–395.

30 C. C. Ho, A. Keller, J. A. Odell and R. H. Ottewill, *Colloid Polym. Sci.*, 1993, **271**, 469–479.

31 Y. Lu, Y. Yin and Y. Xia, *Adv. Mater.*, 2001, **13**, 271–274.

32 C. M. Tseng, Y. Y. Lu, M. S. El-Aasser and J. W. Vanderhoff, *J. Polym. Sci. Part A Polym. Chem.*, 1986, **24**, 2995.

33 C. K. Ober, *Makromol. Chemie. Macromol. Symp.*, 1990, **35–36**, 87.

34 W. Yang, J. Hu, Z. Tao, L. Li, C. Wang and S. Fu, *Colloid Polym. Sci.*, 1999, **277**, 446.

35 D. Wang, V. L. Dimonie, E. David Sudol and M. S. El-Aasser, *J. Appl. Polym. Sci.*, 2002, **84**, 2721.

36 Z. Song, E. S. Daniels, E. D. Sudol, A. Klein and M. S. El-Aasser, *Colloid Polym. Sci.*, 2014, **292**, 645.

37 J. G. Tsavalas and D. C. Sundberg, *Langmuir* 2010, **26**, 6960.

38 B. Jiang, J. G. Tsavalas and D. C. Sundberg, *Langmuir* 2010, **26**, 9408.

39 A. K. Tripathi, J. G. Tsavalas and D. C. Sundberg, *Thermochim. Acta* 2013, **568**, 20.

40 B. J. Lee, A. S. Argon, D. M. Parks, S. Ahzi and Z. Bartczak, *Polymer (Guildf).*, 1993, **34**, 3555.

41 S. Lee and G. C. Rutledge, *Macromolecules*, 2011, **44**, 3096.

42 J. Y. He, Z. L. Zhang, M. Midttun, G. Fonnum, G. I. Modahl, H. Kristiansen and K. Redford, *Polymer (Guildf).*, 2008, **49**, 3993.

43 C. C. W. J. Clarijs and L. E. Govaert, *J. Polym. Sci. Part B Polym. Phys.*, 2019, **57**, 1001.

44 A. S. Argon, *Philos. Mag.*, 1973, **28**, 839.

45 F. M. Capaldi, M. C. Boyce and G. C. Rutledge, *Polymer (Guildf).*, 2004, **45**, 1391.

46 G. A. Medvedev and J. M. Caruthers, *Macromolecules*, 2015, **48**, 788.

47 J. Caruthers and G. Medvedev, in *Polymer Glasses*, ed. C. B. Roth, CRC Press, Boca Raton, FL, 2016, **4**, 106.

48 P. Zhang, D. C. Sundberg and J. G. Tsavalas, *Ind. Eng. Chem. Res.,* 2019, **58**, 21118.

49 J. M. Stubbs and D. C. Sundberg, *J. Polym. Sci. Part B Polym. Phys.,* 2011, **49**, 1583.

50 W. Li, T. Suzuki and H. Minami, *Angew. Chemie - Int. Ed.*, 2018, **57**, 9936.

51 A. Pawlak, A. Galeski and A. Rozanski, *Prog. Polym. Sci.*, 2014, **39**, 921.

52 M. Hashimoto, S. Fujiwara, N. Lin, A. Doi, N. Katayama, J. Ootani and T. Mizuguchi, *Polym. J.*, 2019, **51**, 569.

53 P. F. Liu and X. K. Li, *J. Peridynamics Nonlocal Model.*, 2019, **1**, 3.